



ELSEVIER

Geomorphology 44 (2002) 145–154

GEOMORPHOLOGY

www.elsevier.com/locate/geomorph

A relict landscape in the centre of Fennoscandian glaciation: cosmogenic radionuclide evidence of tors preserved through multiple glacial cycles

Arjen P. Stroeven^{a,*}, Derek Fabel^b, Clas Hättestrand^a, Jon Harbor^c

^aDepartment of Physical Geography and Quaternary Geology, Stockholm University, S-106 91 Stockholm, Sweden

^bSchool of Earth Sciences, The University of Melbourne, Melbourne, Australia

^cDepartment of Earth and Atmospheric Sciences, Purdue University, West Lafayette, IN, USA

Received 19 June 2001; received in revised form 30 August 2001; accepted 6 September 2001

Abstract

The presence of well-developed tors, boulder fields, and weathering mantles in the Parkajoki area of northeastern Sweden, near the centre of Fennoscandian glaciation, has been used to suggest that these landscapes were preserved during all glacial cycles since ice-sheet initiation in the late Cainozoic. This implies that all successive large-scale glaciations must have had frozen bed conditions across this area to allow for subglacial landscape preservation. Cosmogenic ¹⁰Be and ²⁶Al data from three tors and a meltwater channel in the Parkajoki area were used to test this hypothesis of landscape preservation through multiple glacial cycles. Apparent exposure ages of tor summit bedrock surfaces ranging between 79 and 37 ka in an area deglaciated at ~11 ka are consistent with the interpretation of these features as relict landforms that have survived glaciation with little or no erosion. Single nuclide minimum exposure age data require that the tors have survived at least two complete glacial cycles. This estimate is based on (i) the approximate duration of periods of ice sheet cover versus ice free conditions as deduced from the DSDP 607 marine benthic foraminifer oxygen isotope record, in conjunction with (ii) a record of Fennoscandian ice sheet flow traces (and hence, ice sheet extent), and (iii) noting that cosmogenic nuclides are accumulated only during ice free periods. In addition, mean cosmogenic ²⁶Al/¹⁰Be concentration ratios from two of the sites indicate a minimum model total history of 605 ka and a maximum erosion rate of 1.6 m Ma⁻¹. Thus, the numerical ages confirm the overall qualitative interpretation of landscape preservation through multiple glacial cycles. © 2002 Elsevier Science B.V. All rights reserved.

Keywords: Glacial erosion; Relict landscape; Tor; Ice sheet; Cosmogenic radionuclide

1. Introduction

Hättestrand and Stroeven (this issue) describe a nonglacial relict landscape around the Parkajoki river, in the northeastern Swedish lowlands (Fig. 1). For a

site near the centre of Fennoscandian glaciation, it is remarkable that the landscape is characterised by well-developed tors, boulder fields, and weathering mantles, and that the only traces of glaciation are till veneers and meltwater channels. Tors in this area occur typically in summit positions in gneiss or gneissic granite bedrock (Fig. 2). They exhibit extensively weathered and vertical cliff faces that extend at least 0.5 m below the ground surface into the grus.

* Corresponding author. Tel.: +46-8-164230; fax: +46-8-6747895.

E-mail address: arjen@geo.su.se (A.P. Stroeven).

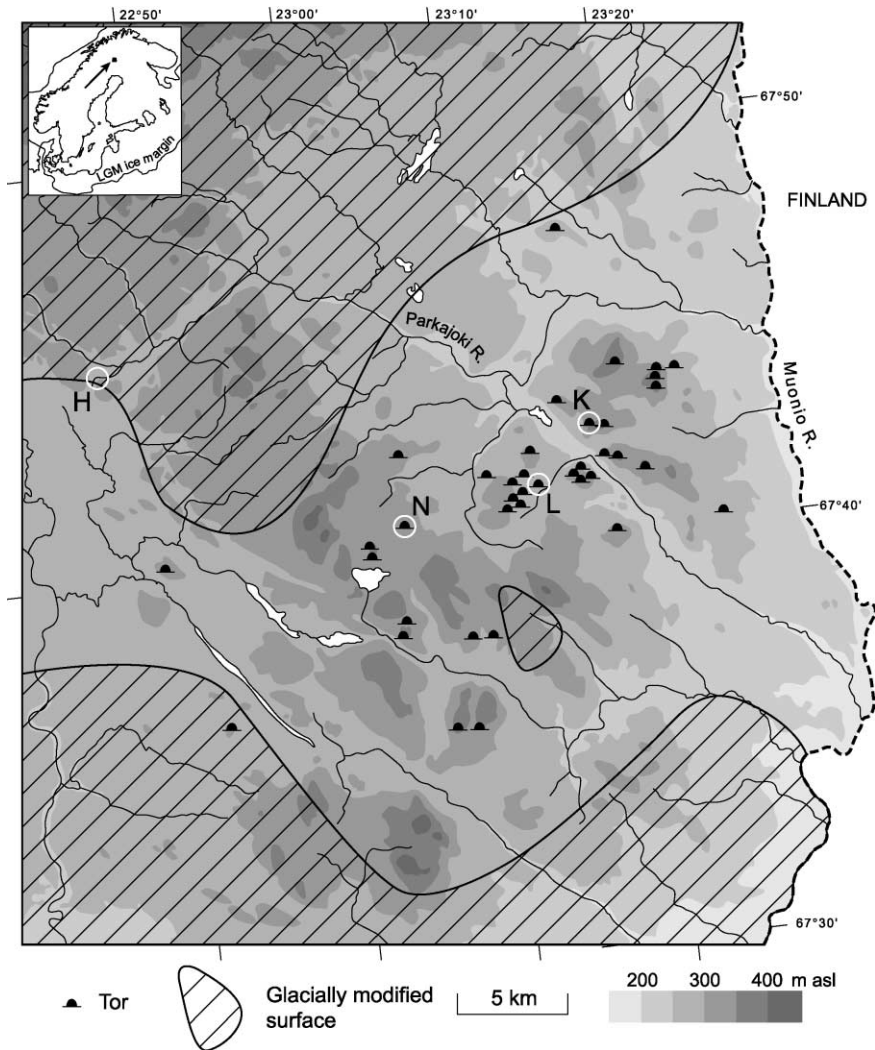


Fig. 1. Location and features of the Parkajoki area. Note that the entire study area has been covered repeatedly by Quaternary ice sheets. The glacially modified surfaces (hatched) contain abundant subglacial landforms, such as drumlins, flutings, and eskers (Hättestrand and Stroeven, this issue). Areas in between the glacially modified surfaces typically lack subglacial landforms, but well-developed tors (hat symbol), boulder fields, weathering mantles, and meltwater landforms, such as lateral meltwater channels, are abundant. Letters refer to the sites discussed in the text: H—Haltiojärvi, K—Kiuhtislompolo, L—Lamuvaara, N—Naakakarhukka (see Table 1).

Tors like those described by Hättestrand and Stroeven (this issue) were probably formed as a result of deep weathering and stripping in preglacial times, with additional sediment removal by mass movement under periglacial conditions in interglacial and interstadial times. If this interpretation is correct, tors in areas known to have been glaciated are truly relict features and provide a measure of the relative inefficiency of glacial erosion in certain locations. Such

areas of little or no erosion also indicate that during multiple glaciations, patches of non-erosive and presumably cold-based ice must have been established repeatedly over the same locations (Hättestrand and Stroeven, this volume). Here, we use cosmogenic nuclide techniques to test the hypothesis that the tors of the Parkajoki area and, by inference, the surrounding landscape, are in fact relict features that have persisted through one or more glacial cycles. If the tors of the



Fig. 2. Sampled tors. (a) Summit surface of the tor at Naakakarhakka. Note the rough weathered bedrock surface (relief ~ 10 cm) and grus remnants. Lens cap for scale. (b) Tor at Lamuvaara with extensive weathering along the closely spaced horizontal joint planes. (c) A 4-m high tor at Kiuhtislompolo developed in gneissic granite with sub-vertical foliation.

Parkajoki area are not relict features, then they should have cosmogenic nuclide exposure ages consistent with the last deglaciation.

2. Methods

Samples for cosmogenic nuclide analysis were collected from summit surfaces of three tors (Fig. 2) and a bedrock outcrop in a meltwater channel. Approximately 24–36 g of pure quartz was separated from each sample using magnetic and heavy liquids separation followed by selective chemical dissolution (Kohl and Nishiizumi, 1992). The quartz was dissolved in HF and HNO₃, and spiked with ~ 0.6 mg ⁹Be carrier. Total Al concentrations in aliquots of the dissolved quartz were quantified by ICP and assigned

a 5% uncertainty. After expelling fluorides in the presence of HClO₄, the Al and Be were separated and purified by ion chromatography and selectively precipitated as hydroxides. The precipitates were oxidised for determination of ¹⁰Be/⁹Be and ²⁶Al/²⁷Al by accelerator mass spectrometry (AMS). Procedural blanks were used to correct measured ratios.

To calculate cosmogenic ages and erosion rates, we used the standard models of Lal (1991) with sea-level, high latitude ($>60^\circ$), isotope production rates of 5.1 ± 0.3 atoms g⁻¹ year⁻¹ (¹⁰Be) and 31.1 ± 1.9 atoms g⁻¹ year⁻¹ (²⁶Al) scaled to altitude and latitude (Stone, 2000). A correction was applied for sample thickness using an attenuation coefficient of 160 ± 10 g cm⁻² and density of 2.7 g cm⁻³ for rock. Uncertainties in single nuclide exposure ages (Table 1) represent one standard error in AMS counting statistics, uncertain-

Table 1

Cosmogenic radionuclide data and interpretations for three tor locations (99-01, 99-04 and 99-06) and one fluvial meltwater channel location (99-07) in the Parkajoki area, northeastern Sweden

Sample	Location	Elevation (m a.s.l.)	^{10}Be (10^5 atom g^{-1}) ^a	^{26}Al (10^5 atom g^{-1}) ^a	$^{26}\text{Al}/^{10}\text{Be}$	Single nuclide		Paired nuclide				
						Minimum age (ka)		Minimum age (ka)		Minimum total history (ka)	Maximum erosion rate (m Ma^{-1})	Minimum DSDP 607 total history (ka)
						^{10}Be	^{26}Al	Exposure	Burial			
99-01	Naakakar- hakka	360	3.84 ± 0.17	20.50 ± 0.98	5.34 ± 0.35	79 ± 17	70 ± 15	85	216	301	1.9	485
99-04	Lamuvaara	300	3.08 ± 0.14	15.78 ± 1.14	5.12 ± 0.44	64 ± 14	54 ± 12	71	301	372	1.4	765
	Mean of 99-01 and 99-04		3.46 ± 0.16	18.14 ± 1.06	5.24 ± 0.39	71 ± 16	62 ± 14	78	257	335	1.6	605
99-06	Kiuhtislom- polo	350	1.82 ± 0.11	–	–	37 ± 8	–	–	–	–	–	–
99-07	Haltiojärvi	280	0.55 ± 0.08	3.31 ± 0.49	6.06 ± 1.3	11 ± 3	11 ± 3	NA	NA	NA	NA	NA

^a Samples were collected at latitude $>67^\circ\text{N}$ and measured nuclide concentrations have been normalized to sea level using Stone (2000).

ties in total Al measurement by ICP (5%), radioactive decay rates (8%), and absolute production rates (20%), with each uncertainty added in quadrature.

The cosmogenic nuclide data are interpreted in three ways. First, we calculate minimum limiting single nuclide ages and maximum limiting single nuclide erosion rates. This represents the simplest interpretation of the data, as it assumes continuous exposure (i.e., no burial by ice). Second, we consider the ^{10}Be and ^{26}Al data together and calculate minimum limiting total exposure and shielding (burial) duration, closely following Bierman et al. (1999). Finally, we calculate the minimum total history required to produce the exposure and shielding duration for the tors, using the DSDP 607 marine benthic foraminifer oxygen isotope record (Raymo et al., 1989; Ruddiman et al., 1989; Lazarus et al., 1995) as a proxy for the approximate duration of periods of ice-sheet cover versus ice-free conditions.

3. Results and interpretations

3.1. Single nuclide exposure ages and erosion rates

The calculated ^{10}Be and ^{26}Al single nuclide ages for samples 99-01 and 99-04 (Table 1) are internally inconsistent, indicating that these samples must have been partly or completely shielded from cosmic rays during and/or after initial exposure. During periods of complete shielding, by burial under an ice sheet for example, no cosmogenic nuclides are produced and ^{26}Al and ^{10}Be concentrations inherited from prior cosmic ray exposure diminish by radioactive decay. ^{26}Al (half-life = 705 ka [10^3 years]) decay is relatively rapid with respect to ^{10}Be (half-life = 1500 ka) forcing the $^{26}\text{Al}/^{10}\text{Be}$ ratio of a sample to decrease exponentially over time (Lal and Arnold, 1985; Klein et al., 1986). On a graph of ^{10}Be concentration versus $^{26}\text{Al}/^{10}\text{Be}$, a shielded sample plots below the area termed the 'steady state erosion island' (Lal, 1991) bounded by the trajectory of non-eroding continuous exposure and the trajectory of steady-state erosion end points (Fig. 3; after Lal, 1991; modified from Klein et al., 1986). For an explanation of the ^{10}Be concentration versus $^{26}\text{Al}/^{10}\text{Be}$ plot, we refer the reader to Bierman et al. (1999), while Granger and Muzikar (2001) provide the relevant equations and a detailed account of the

problems and limitations of using the plot for interpreting ^{10}Be and ^{26}Al measurements.

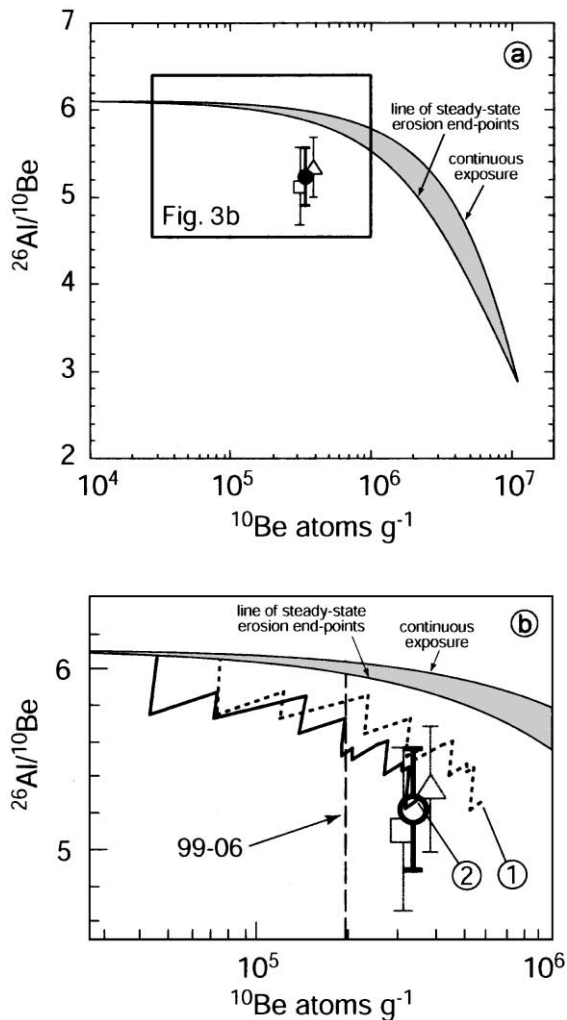
3.2. Paired nuclide data

The position of the two tor samples with internally inconsistent ^{10}Be and ^{26}Al ages below the steady-state curves (Fig. 3) does not, on its own, define a single unique exposure/burial history. Following Bierman et al. (1999), it is possible to delimit three possible general classes of exposure and burial history. The first class consists of samples that experienced continuous exposure followed by burial sufficient to shield completely the sample from cosmogenic nuclide production. This provides the shortest total sample history consistent with measured concentrations. Assuming this case, we calculate the minimum exposure and burial duration consistent with measured ^{10}Be and ^{26}Al concentrations (Table 1). Following Bierman et al. (1999), we use an initial rapid exposure of a sample containing no cosmogenic nuclides, followed by a period of burial, and thus derive minimum limits for total exposure history from the sum of the exposure and burial times (Table 1, minimum total history).

The second general class of exposure/burial histories consists of continuous exposure under partial shielding conditions. In our case, we might argue that the samples became recently fully exposed and received cosmic ray dosing under a continuous cover of regolith, till, snow or ice. Production rates of ^{26}Al and ^{10}Be decrease exponentially with depth (Lal, 1991; Granger and Smith, 2000), however this variation affects ^{26}Al and ^{10}Be alike and therefore has no effect on their production rate ratio. Partial shielding does, however, reduce the effective nuclide production, and hence the nuclide concentration. Because our samples would have experienced complete shielding under thick ice during periods of Fennoscandian glaciation, a continuous partially shielded exposure history is unlikely. However, partial shielding during interglacial periods of exposure may have influenced the nuclide inventory and may therefore change the position of the sample along the x -axis of the ^{10}Be concentration versus $^{26}\text{Al}/^{10}\text{Be}$ ratio plot (Fig. 3).

The third general class of exposure/burial histories consists of non-steady state erosion events, which could include processes such as shallow landslides or

bedrock spallation. In non-steady state erosion events, accumulated nuclides are rapidly removed without affecting the $^{26}\text{Al}/^{10}\text{Be}$ ratio, but again reducing the nuclide concentration in a sample (Small et al., 1997). Clearly, complex combinations of these three idealised exposure/burial histories are possible (such as repeated exposure and burial), and these will result in sample positions that are shifted left from the steady state exposure trajectories (Bierman et al., 1999; Fabel and Harbor, 1999). As demonstrated by Bierman et al. (1999) a complex history of alternating constant exposure and burial times leads to an oscillatory trajectory, with a central tendency controlled by the ratio of burial to exposure and an oscillation amplitude controlled by the duration of burial and exposure.



Here, we take the complex exposure model further. The Fennoscandian ice sheet glaciation history for marine isotope stages 5d–2 is now well established (cf. Kleman et al., 1997; Hättestrand, 1998; Boulton et al., 2001), and forms the basis for postulating ice sheet configuration and duration during the Plio-Pleistocene period of enhanced North Atlantic glaciation (Kleman and Stroeven, 1997; Jansen et al., 2000). Reconstructed Mountain ice sheet and Fennoscandian ice sheet configurations based on flow traces (Kleman et al., 1997) in conjunction with the DSDP 607 marine benthic foraminifer oxygen isotope record of global ice volume as a proxy for the duration of periods of ice sheet cover versus ice free conditions (Kleman and Stroeven, 1997) provide us with a possible complex exposure and burial history for the study area. Our sample sites lie within the area covered by Mountain ice sheets (Kleman and Stroeven, 1997) and we used these authors $\delta^{18}\text{O}$ limit for this style of ice sheet to divide the DSDP 607 record into periods of ice sheet cover ($\delta^{18}\text{O} > 3.7\text{‰}$) versus ice-free conditions ($\delta^{18}\text{O} \leq 3.7\text{‰}$). The minimum total history for the tors was

Fig. 3. Plot of ^{10}Be concentration versus $^{26}\text{Al}/^{10}\text{Be}$. Samples exposed at the surface should fall in the area (shaded grey) known as the 'steady-state erosion island' (Lal, 1991), which has as limiting envelopes the curve of steady-state erosion end points and the curve of continuous exposure. (a) Tor samples collected at Naakakarhukka (triangle) and Lamuvaara (square) plot below the steady-state erosion island indicating burial during their total histories. The solid circle marks the mean value derived from the two tors. Error bars are 1σ analytical uncertainty. (b) Detail of modelled complex exposure trajectories. The measured values for the two tors are shown in grey and the mean value by the open black circle. The zigzag trajectories show the modelled complex exposure trajectories of a sample forced along the ice-free/ice-covered history provided by the DSDP 607 marine oxygen isotope proxy glacial record. The dashed trajectory shows the model result for continuous, unshielded exposure during ice-free periods. Note that the modelled complex history overestimates the ^{10}Be concentration (1). The solid trajectory terminates at the correct ^{10}Be concentration (2) and was derived using the same complex history as for (1) but with partial shielding of 83 g cm^{-2} during all exposure periods except the last 11 ka. A minimum total history of 605 ka is required to achieve better than 1% concordance between the $^{26}\text{Al}/^{10}\text{Be}$ ratio of the modelled sample and the mean ^{10}Be concentration value derived from the two tors. The measured ^{10}Be concentration of the third tor sample (99-06) falls somewhere on the dashed line (arrowed). If it was subject to the same history as the other tor samples it requires increased partial shielding to account for the lower ^{10}Be concentration.

modelled by starting the initial exposure of the sample at the beginning of an ice-free period in the past and using the DSDP 607 record to limit subsequent burial and exposure periods until the present. The starting point of the model was changed until the modelled $^{26}\text{Al}/^{10}\text{Be}$ ratio differed by less than 1% from the mean of the measured ratios. However, because calculated ^{10}Be and ^{26}Al concentrations exceeded the measured concentrations (dashed trajectory, Fig. 3B), the model was repeated with partial shielding during exposure periods to reach concordance in modelled and measured nuclide concentrations (solid trajectory, Fig. 3B). Using a marine oxygen isotope curve to infer ice cover history for a specific land area may overestimate the duration of ice cover (Porter, 1989), hence the calculated total history is a minimum estimate. Three exposure/burial models (i.e. constant exposure followed by burial, instantaneous erosion, and complex exposure/burial) form the framework for our construction and interpretation of limiting sample histories.

4. Discussion

The exposure ages calculated from the single nuclide data are minimum ages because they assume the samples were constantly exposed at the surface, had no inherited nuclide concentrations from a previous exposure history, and experienced no erosion or coverage by snow. Erosion of the sampled surface or undetected shielding would lower nuclide concentrations and yield calculated exposure ages younger than the true exposure age. The sample collected from the meltwater channel at Haltiojärvi yields an exposure age of 11 ± 3 ka for both ^{10}Be and ^{26}Al (Table 1). This concordance indicates continuous exposure of the sampled surface. Because of its location in a meltwater channel, it is unlikely that this sample site was ever exposed to cosmic rays prior to the last glaciation and we interpret the exposure age as the deglaciation age for this area. This timing of deglaciation is consistent with existing models for deglaciation in northern Fennoscandia (Boulton et al., 2001; Kleman and Strömberg, in press). The ^{10}Be single nuclide apparent exposure ages of the three tor samples are significantly older than this deglaciation age (79 ± 17 , 64 ± 14 and 37 ± 8 ka; Table 1), indicating that the tor surfaces have

nuclide concentrations inherited from earlier exposure. At minimum, these surfaces have survived the last two glacial cycles. Using the DSDP 607 timescale, the penultimate ice-free period (100–93 ka, Marine Isotope Stage 5c; cf. Kleman and Stroeven, 1997) combined with continuous exposure since last deglaciation, yields a total exposure length ($11 + 7$ ka) that is insufficient to account for the minimum exposure ages. To obtain the ^{10}Be exposure age for Kiuhtislompolo of 37 ± 8 ka, requires accumulated exposure during three ice-free periods with intervening periods of ice cover. The last ice-free period, which satisfies this scenario, occurs at ~ 128 ka. The exposure ages for samples collected from Lamuvaara and Naakakarhakka require seven ice-free periods dating back to 261 ka. These total exposure histories from the ^{10}Be data are minimum estimates because they do not include nuclide decay, and hence lowering of nuclide concentrations, during the intervening periods of burial by ice. The ^{26}Al exposure ages for Lamuvaara and Naakakarhakka are less than corresponding ^{10}Be ages (Table 1), confirming that the samples experienced episodes of burial.

Using the ^{10}Be and ^{26}Al data and an assumption of single exposure followed by continuous burial yields minimum total sample histories of 301 and 372 ka for Naakakarhakka and Lamuvaara, respectively, with a mean of 335 ka (Table 1). The maximum erosion rates calculated for these two sites are 1.9 and 1.4 m Ma^{-1} , respectively (mean = 1.6 m Ma^{-1}). These results indicate that the summit surfaces of the two tors are old and stable and that the exposure histories are complex, including much longer periods of shielding than exposure (Table 1). However, the minimum total history model assumes that the sampled surfaces have only recently been exposed, whereas it is likely that these surfaces were exposed throughout the Holocene. The longer the period of recent continuous exposure, the more the calculated minimum total exposure histories would underestimate the true age of the sampled surfaces. Given our deglaciation age of 11 ka at Haltiojärvi, and assuming that the Naakakarhakka and Lamuvaara sites have also been exposed since this time, the recalculated total exposure histories would increase to 383 and 428 ka, respectively. However, more complete adjustments are needed to reconcile ice sheet records with the cosmogenic radionuclide burial and exposure history.

Bierman et al. (1999) showed that if exposure and burial alternated, measured nuclide concentrations could be compatible with any number of scenarios. Using the DSDP 607 oxygen isotope data as our preferred scenario (Kleman and Stroeven, 1997) provides us with one possible complex exposure and burial history for the two tor samples. Although it is tempting to model the complex histories of these samples separately, they are statistically indistinguishable ($\pm 1\sigma$) so we use the mean of the measured ^{10}Be and ^{26}Al values (Table 1). To obtain the mean $^{26}\text{Al}/^{10}\text{Be}$ value of 5.24 ± 0.39 for Naakakarhakka and Lamuvaara using the DSDP 607 burial and exposure history yields a total history of 605 ka (minimum estimate). This history includes 11 exposure and 10 burial events with a combined duration of 128 and 477 ka, respectively. Although the modelled $^{26}\text{Al}/^{10}\text{Be}$ ratio differs by less than 1% from the calculated mean value, the modelled ^{10}Be concentration of 5.79×10^5 atoms g^{-1} overestimates the measured concentration by 167% (dashed trajectory, Fig. 3B). This discrepancy indicates that the complex history includes partial shielding during periods of exposure. The modelled ^{10}Be concentration and $^{26}\text{Al}/^{10}\text{Be}$ ratio are concordant with the calculated mean value if we assume partial shielding of 83 g cm^{-2} during all ice-free periods except for the last 11 ka (Fig. 3B).

If we assume that contemporary meteorological data (Raab and Vedin, 1995) are representative for all ice-free periods, snow is responsible for only 16% of the partial shielding. For the period between 1961 and 1990, the mean maximum snow depth in our study area was 80 cm and snow covers the ground on average 200 days per year (Raab and Vedin, 1995). This equates to an annual shielding value of 13 g cm^{-2} (assuming a density of 0.3 g cm^{-3}) which is equivalent to shielding by $\sim 5 \text{ cm}$ of rock. Assuming that similar snow conditions existed during past interglacials, would lead to an increase in calculated ages of $\sim 5\%$ compared to an exposure history which omits snow cover. This level of change in calculated ages does not have a significant impact on the overall conclusions drawn from the results. Increased snow depth or cover duration in the past would further increase calculated single nuclide ages. The true effect of shielding by snow is probably much less than calculated for average conditions as snow preferentially accumulates in depressions, leaving topographic rises

(i.e. tors) relatively devoid. Hence, in calculating limiting single nuclide exposure ages (Table 1), we assumed an absence of snow.

Strong horizontal jointing and the presence of thin slabs of bedrock proximal to the weathered summit surfaces of the three tors (Fig. 2) may indicate a combination of glacial-unloading induced spallation and aerially restricted plucking and re-deposition of rock slabs, rather than removal of a weathering mantle or till cover, to explain the partial shielding indicated by the measured nuclide concentrations. An alternative to the removal of bedrock ($\sim 31 \text{ cm}$ thick with a density of 2.7 g cm^{-3}) is the removal of an overlying weathering mantle or till ($\sim 42 \text{ cm}$ thick with a density of 2.0 g cm^{-3}) during or immediately prior to the last ice over-riding (burial) event. Survival until recently of such relatively thin bedrock or till overburden through multiple glaciations would confirm large-scale non-erosive ice in this area.

Given the similarity of outcrop characteristics and its proximity to the other two tor sites, the exposure and burial history of the sample collected on the summit of Kiuhtislompolo is likely to have been similar. If this is the case, the much lower ^{10}Be concentration measured in this sample (Table 1) probably indicates more significant partial shielding. Using the same DSDP 607 model history as for the other two tors, the thickness of bedrock removed to account for the measured ^{10}Be concentration is $\sim 69 \text{ cm}$. In the absence of ^{26}Al data for this sample, it is impossible to verify this estimate or the minimum total exposure history for this site.

The complex exposure/burial model results depend on the assumption that the DSDP 607 marine benthic foraminifera oxygen isotope record of global ice volume is a proxy for the approximate duration of periods of ice sheet cover versus ice free conditions in our field area, and that Kleman and Stroeven's (1997) slicing of this record along $\delta^{18}\text{O}$ limits is generally valid. Although the details of any reconstruction are debatable, the overall conclusions of this study depend only on the overall framework and scale of the proxy relationship. Even if we only consider ice to have occupied the field area during periods when $\delta^{18}\text{O} > 4.5\text{‰}$ (i.e. Kleman and Stroeven's, 1997 Fennoscandian ice sheet scenario) the modelled total history still spans 590 ka. Going even further, if we were to reject the idea of using the DSDP 607 record to

constrain periods of ice cover, the minimum total histories determined from the cosmogenic nuclide data alone would still require a general conclusion of landscape preservation through at least the last ice-sheet overriding event in this area.

In summary, the reconstructed minimum total histories and maximum limiting erosion rates calculated from the paired ^{10}Be and ^{26}Al measurements imply that the late Quaternary Fennoscandian ice sheets were ineffective as erosional agents within the Parkajoki river study area. These results corroborate Hättestrand and Stroeven's (this volume) inferences of tor-landscape preservation through Plio-Pleistocene glacial cycles. One factor contributing to this preservation of landforms in the Parkajoki area is its location beneath or close to the LGM ice divide position. This is because the horizontal component of ice flow, and, hence erosive capacity, is negligible for this and previous maximum positions of full-scale Fennoscandian glaciations in this area. Helmens et al. (2000) also invoke this relationship to explain the preservation of interglacial stratigraphy at nearby Sokli. However, for most of the glaciation history, including inception, build up, and decay, the ice divide was located elsewhere. Hence, we infer that ice sheets remained consistently cold-based over the Parkajoki area, regardless of their evolution and outline, to account for the tor preservation. Hättestrand and Stroeven (this volume) explain how cold-based ice might have remained positioned over the Parkajoki area lowland terrain for different palaeoglaciological settings. These results highlight the polythermal nature of Plio-Pleistocene ice sheets and suggest that inclusion of cold-based regions in numerical ice sheet models is of key importance to the predictive success of these models and general circulation models of climate that depend on reconstructions of ice sheet extent and morphology.

5. Conclusions

Apparent exposure ages of three tor summit bedrock surfaces in the northern Swedish lowlands, at the centre of Fennoscandian glaciation, range between 79 and 37 ka. Using DSDP 607 marine benthic foraminifer oxygen isotope record as a proxy for the duration of periods of ice sheet cover versus ice free conditions, and noting that cosmogenic nuclides are only

accumulated during ice free periods, mean cosmogenic $^{26}\text{Al}/^{10}\text{Be}$ concentration ratios from two of the sites indicate a minimum total history of 605 ka and a maximum erosion rate of 1.6 m Ma^{-1} . Thus, the numerical ages confirm the overall qualitative interpretations of these features as relict landforms that have survived glaciation with little or no erosion and, hence, of long-term landscape preservation.

Acknowledgements

Samples were processed at the University of Melbourne and the Purdue Rare Isotope Measurement Laboratory (PRIME Lab), Purdue University. Funding for this research was provided by the Swedish Natural Science Research Council, the US National Science Foundation (Grant OPP 9818162), PRIME Lab (seed grant), and the Swedish Society for Anthropology and Geography. This work was completed while the New Zealand–United States Educational Foundation supported JH as a Fulbright Senior Scholar. We thank two journal reviewers (Michael Thomas and Andrew Plates) and Ola Fredin for insightful comments.

References

- Bierman, P.R., Marsella, K.A., Patterson, C., Davis, P.T., Caffee, M., 1999. Mid-Pleistocene cosmogenic minimum-age limits for pre-Wisconsinan glacial surfaces in southwestern Minnesota and southern Baffin Island: a multiple nuclide approach. *Geomorphology* 27, 25–39.
- Boulton, G.S., Dongelmans, P., Punkari, M., Broadgate, M., 2001. Palaeoglaciology of an ice sheet through a glacial cycle: the European ice sheet through the Weichselian. *Quaternary Science Reviews* 20, 591–625.
- Fabel, D., Harbor, J., 1999. The use of in-situ produced cosmogenic radionuclides in glaciology and glacial geomorphology. *Annals of Glaciology* 28, 103–110.
- Granger, D.E., Muzikar, P.F., 2001. Dating sediment burial with in situ-produced cosmogenic nuclides: theory, techniques, and limitations. *Earth and Planetary Science Letters* 188, 269–281.
- Granger, D.E., Smith, A.L., 2000. Dating buried sediments using radioactive decay and muogenic production of ^{26}Al and ^{10}Be . *Nuclear Instruments and Methods in Physics Research B: Beam Interactions with Materials and Atoms* 172, 822–826.
- Hättestrand, C., 1998. The glacial geomorphology of central and northern Sweden. *Sveriges Geologiska Undersökning, Ca* 85: 47 pp.
- Hättestrand, C., Stroeven, A.P., 2002. A relict landscape in the centre of Fennoscandian glaciation: Geomorphological evidence of minimal Quaternary glacial erosion. *Geomorphology* in press.

- Helmens, K.F., Rasanen, M.E., Johansson, P.W., Jungner, H., Korjonen, K., 2000. The Last Interglacial–Glacial cycle in NE Fennoscandia: a nearly continuous record from Sokli (Finnish Lapland). *Quaternary Science Reviews* 19, 1605–1623.
- Jansen, E., Fronval, T., Rack, F., Channell, J.E.T., 2000. Pliocene–Pleistocene ice rafting history and cyclicity in the Nordic Seas during the last 3.5 Myr. *Paleoceanography* 15, 709–721.
- Klein, J., Giegengack, R., Middleton, R., Sharma, P., Underwood, J.R., 1986. Revealing histories of exposure using in situ produced ^{26}Al and ^{10}Be in Libyan desert glass. *Radiocarbon* 28, 547–555.
- Kleman, J., Stroeven, A.P., 1997. Preglacial surface remnants and Quaternary glacial regimes in northwestern Sweden. *Geomorphology* 19, 35–54.
- Kleman, J., Strömberg, B., in press. Deglaciation of Fennoscandia. In: Gerrard, J. (Ed.), *Encyclopedia of Quaternary Science*, Kluwer Academic Publishers.
- Kleman, J., Hättestrand, C., Borgström, I., Stroeven, A.P., 1997. Fennoscandian paleoglaciology reconstructed using a glacial geological inversion model. *Journal of Glaciology* 43, 283–299.
- Kohl, C.P., Nishiizumi, K., 1992. Chemical isolation of quartz for measurement of in situ-produced cosmogenic nuclides. *Geochimica et Cosmochimica Acta* 56, 3586–3587.
- Lal, D., 1991. Cosmic ray labeling of erosion surfaces: in situ nuclide production rates and erosion models. *Earth and Planetary Science Letters* 104, 424–439.
- Lal, D., Arnold, J.R., 1985. Tracing quartz through the environment. *Proceedings of the Indian Academy of Sciences (Earth and Planetary Sciences)* 94, 1–5.
- Lazarus, D., Spencer-Cervato, C., Pika-Biolzi, M., Beckmann, J.P., Salis, K., Hilbrecht, H., Thierstein, H., 1995. Revised Chronology of Neogene DSDP Holes from the World Ocean. *Ocean Drilling Program Technical Report*, 24.
- Porter, S.C., 1989. Some geological implications of average Quaternary glacial conditions. *Quaternary Research* 32, 245–261.
- Raab, B., Vedin, H., 1995. *Climate, Lakes and Rivers*. National Atlas of Sweden. SNA Publishing, Stockholm, 176 pp.
- Raymo, M.E., Ruddiman, W.F., Backman, J., Clement, B.M., Martinson, D.G., 1989. Late Pliocene variation in northern hemisphere ice sheets and North Atlantic deep water circulation. *Paleoceanography* 4, 413–446.
- Ruddiman, W.F., Raymo, M.E., Martinson, D.G., Clement, B.M., Backman, J., 1989. Pleistocene evolution: northern hemisphere ice sheets and North Atlantic Ocean. *Paleoceanography* 4, 353–412.
- Small, E.E., Anderson, R.S., Repka, J.L., Finkel, R., 1997. Erosion rates of alpine bedrock summit surfaces deduced from in situ ^{10}Be and ^{26}Al . *Earth and Planetary Science Letters* 150, 413–425.
- Stone, J.O., 2000. Air pressure and cosmogenic isotope production. *Journal of Geophysical Research* 105, 23753–23759.